Estimation of Nonhomogeneous Prestrain in a Continuum Ligament Model

William Zaylor

November 16, 2018

Chapter 1

Introduction

1.1 Background

Computational joint models are important tools that can be used to better understand joint mechanics and the conditions that can alter joint behavior. Knee models have been used to evaluate joint behavior that is difficult or impossible to measure *in-vitro* or *in-vivo*. Previous studies have used knee models to evaluate the joint's mechanics for healthy (Blankevoort and Huiskes, 1996; Pea et al., 2006), injured (Ali et al., 2016), and surgically repaired (Thompson et al., 2011; Amiri et al., 2012; Salehghaffari and Dhaher, 2015; Smith et al., 2016b) joint conditions. Specificmen-specific knee models have been shown to more accurately predict the joint's behavior.

Specimen-Specific Knee Models

Specimen-specific knee models are composed of specimen-specific geometry and material properties. The geometry is normally generated from MR imaging, and material properties for hard and soft tissues are determined with either experimentation (Gardiner and Weiss, 2003) or inverse modeling (Blankevoort and Huiskes, 1996; Baldwin et al., 2009; Ewing et al., 2015; Harris et al., 2016). The joint's kinematics and contact mechanics have been shown to be sensitive to variations in ligament properties under passive (Baldwin et al., 2009; Dhaher et al., 2010; Ewing et al., 2015) and dynamic (Smith et al., 2016a) joint loading, therefore specimen-specific ligament properties are needed to model the joint's behavior (Ewing et al., 2015). In addition to constitutive properties, ligament prestrain must also be defined because each ligament's geometry is defined from MR images, where the ligaments may be under an unknown amount of load (Weiss and Gardiner, 2001; Maas et al., 2016). Specimen-specific prestrain is important to define because joint

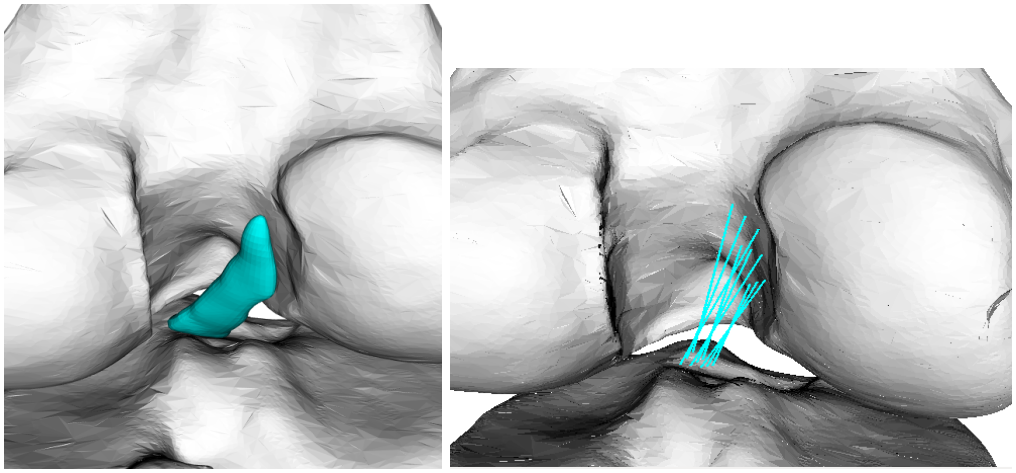

Figure 1.1: A comparison of the anterior cruciate ligament (ACL) modeled as a (left) continuum and (right) a bundle of nine individual springs arranged across the ligament's insertion site.

kinematics have been shown to more sensitive to prestrain than stiffness (Baldwin et al., 2009). It has been shown that prestrain is not uniform throughout a ligament (Hull et al., 1996; Gardiner et al., 2001) , and the way that prestrain is applied to a ligament varies depending on the ligament representation.

Ligament Representation and Prestrain Definition

Ligaments are commonly represented as either bundles of nonlinear uniaxial springs (Blankevoort and Huiskes, 1991; Baldwin et al., 2009; Amiri et al., 2012; Kia et al., 2016), or as a solid continuum (Gardiner and Weiss, 2003; Pea et al., 2006; Dhaher et al., 2010) (Figure 1.1). Studies that utilize spring ligament representations can simulate nonhomogeneous prestrain in a ligament by varying the prestrain in each spring that composes a specific ligament. With the exception of Gardiner and Weiss (2003), specimen-specific nonhomogeneous prestrain is not utilized in continuum ligament models. Studies that utilize continuum ligament representations either apply uniform prestrain (Limbert et al., 2004; Song et al., 2004; Beidokhti et al., 2017), or nonhomogeneous prestrain based on values reported in the literature (Pea et al., 2006; Dhaher et al., 2010), where prestrains are derived from a combination of experimental studies and results of inverse modeling studies that utilize spring ligament models.

There are few studies that evaluate the effects of ligament representation on the model's performance, and improvements can be made to the studies that have addressed this topic. Beidokhti et al. (2017) used inverse modeling to generate comparable spring and continuum ligament models. The two types of models were considered equivalent if they yielded joint forces that were similar to experimentally measured values, however it was not shown that the spring and continuum ligament models yielded similar ligament forces at at a given joint position. Additionally, the prestrain definition may not be equivalent between the spring

and continuum ligament representations. Conversely, Orozco et al. (2018) applied similar prestrain to their spring and continuum ligament models, however prestrain was uniformly applied throughout each ligament.

1.2 Overview

A calibrated knee model that represents ligaments as springs could be used to estimate specimen-specific nonhomogeneous prestrain in continuum representations of ligaments. Lu et al. (2007) estimated the prestrain in blood vessels using an inverse elastostatics approach, where the deformed state of the geometry and forces were known, and the stress-free shape of the geometry was estimated. The overall purpose of this work is to (1) develop an approach to estimating specimen-specific nonhomogeneous prestrain in ligaments that are represented as a continuum and (2) compare the performance of the continuum ligament representation to an equivalent spring ligament representation.

There are four specific aims that are used to work towards the purpose of this work. The first aim is to collect specimen-specific force-displacement data under novel loading conditions. These data will be used in an inverse modeling scheme to estimate each specimen's ligament slack lengths. Experimental data will be reduced to identify loading conditions that specifically load individual ligaments, and a subset of loading conditions that load all of the modeled ligaments. The results of the other specific aims will be used to support the estimation of subject-specific nonhomogeneous ligament prestrain in ligaments modeled as a continuum. Force results from the specimen-specific forward kinematics model will be used to define boundary conditions for an inverse elastostatics analysis, and the reduced set of loading conditions will be used to evaluate the calibrated continuum ligament models.

This work will develop and evaluate an approach to defining specimen-specific nonhomogeneous prestrain in ligaments modeled as a continuum. This approach could be used improve knee models that are used to evaluate ligament injury, and offer a better comparison between knee models that represent ligaments as springs and a continuum.

1.2.1 Specific Aims

Experimental Testing

Experimental testing was conducted to collect specimen-specific force-displacement data and MR images for two specimens. These tests applied novel loading that was designed to remove articular contact which focuses the joint's force-displacement behavior on the soft tissue restraints. The applied joint forces and the corresponding joint kinematics were measured throughout testing. The MR imaging provides the data

necessary to create specimen-specific geometry, and the measurements taken during preparation and testing will provide the data necessary to simulate the experimental conditions.

Status: Complete

Contribution: Data necessary to create specimen-specific models and simulate the experimental tests.

Inverse Modeling

Inverse modeling was used to estimate specimen-specific ligament slack-lengths. Use of an experimentally novel joint state and joint loads allows for joint contact to be neglected in the computational model, and may focus the joint's force-displacement behavior on the ligaments. Neglecting contact enables the use of a computationally efficient forward kinematics model, which is used in an inverse modeling scheme to estimate ligament slack-length. This will provide a calibrated model that recreates the experimental conditions.

Status: Complete

Contribution: A novel approach to using inverse modeling to estimate ligament properties.

Dataset Reduction

The purpose of this aim is to determine (1) experimental loading conditions that target a small set of ligaments and (2) define a subset of the experimental tests that target all of the modeled ligaments. The experiments applied five different loading conditions at four different flexion angles for a total of twenty tests. Ligament recruitment varies with the loading condition and flexion angle. The specimen-specific geometry and kinematics can be used to estimate ligament length throughout each test, and these length measurements can be used to estimate which ligaments are recruited during specific tests without defining ligament slack lengths.

Status: Incomplete

Contribution: A set of experimental tests that can be used to evaluate the continuum ligament model's performance.

Continuum Ligament Prestrain

This aim will use an inverse elastostatic analysis to estimate the undeformed geometry of individual ligaments. To evaluate the performance of this method, experimental

Status: Incomplete

Contribution: An approach to defining specimen-specific nonhomogeneous prestrain in a continuum ligament model.

Chapter 2

Distraction Experiment

2.1 Introduction

Laxity tests are used by physicians to assess the integrity of specific ligaments. These tests can involve the physician moving the joint to a specific position and manually applying loads to the joint. Different tests are used for specific ligaments, and the physician assess the amount of joint motion and restraint that is provided (or not provided) by the targeted ligament. In a research setting, similar laxity-style tests are conducted on cadaveric specimens with custom fixtures (**?**Walker et al., 2014; Rachmat et al., 2016)CITATIONS, or six degree-of-freedom robots CITATIONS. Previous work has used physical experiments to quantify the effect of injury CITATION, and different techniques for ligament reconstruction CITATION, joint replacement CITATION,

Experimental data were collected for use in the inverse modeling scheme described in chapter 4. The purpose of the distraction experiments is to collect specimen-specific kinematic and kinetic data under traditional laxity-style loads, and novel distraction laxity-style loads. The traditional laxity-style loads are meant to simulate clinical tests that a physician may use to assess the integrity of specific ligaments. For a given joint position, the

This section describes the experimental protocol that was used to test specimens under traditional and distraction laxity-style tests.

2.2 Methods

2.2.1 Initial Specimen Preparation and Testing

Experimental tests were conducted on two knee specimens (AGE, BMI). The specimens were initially prepared following the OpenKnee(s) protocol (Erdemir, 2016). In short, whole leg specimens from femoral head to foot were initially dissected by removing the soft tissue proximal and distal to the knee, leaving soft tissues intact from 8 cm proximal to the joint line to 8 cm distal. To facilitate model generation, three registration markers were fixed to the femur and tibia (six markers total) approximately 8 cm proximal and distal to the joint line, respectively. Optoelectronic sensors were fixed to the femur and tibia, and the position and orientation of the sensors was measured with an optoelectronic camera system (Optotrak, Northern Digital Inc., Waterloo, Ontario, Canada). Osseous landmarks (medial and lateral femoral epicondyles, femoral head, medial and lateral tibial plateau, and the medial and lateral malleolus) and ten points around each registration marker were digitized. After digitization, the tibia and femur were cut approximately 19 cm proximal and distal to the joint line, respectively. The specimen was them MR imaged. Following MR imaging, the femur and tibia were potted into fixtures that are used to mount to the robot.

A six degree-of-freedom simVITRO^{TM}robot (Cleveland Clinic, Cleveland, OH) was used to apply laxity style loading to the specimen. Following this testing, and orthopedic surgeon dissected the skin, muscle, patella, and menisci, leaving the ligament structures intact. Note the osteoarthritis. The laxity-style tests were performed again on the now cleaned specimen. These tests were performed to increase the amount of data that was collected. The details of these tests are not described here because they do not relate to the distraction testing.

2.2.2 Distraction Testing

The specimens were dissected again following the intact and cleaned testing. An orthopedic surgeon

2.3 Results

Chapter 3

Inverse Modeling

3.1 Introduction

Inverse modeling is normally used to estimate ligament properties using computational knee models and experimental laxity tests (Blankevoort and Huiskes, 1996; Baldwin et al., 2012; Ewing et al., 2015; Harris et al., 2016). These methods assume that for a given joint position the external joint forces balance with the internal ligament and contact forces (Blankevoort and Huiskes, 1996). This approach uses optimization to estimate the ligament properties that minimize the residual model and experimental values. Due to the need to model joint contact, these methods use forward dynamics models because joint contact forces have been shown to sensitive to kinematic errors (Fregly et al., 2008; Yao et al., 2008).

Adjusting experimental conditions to remove articular contact would focus the joint's force-displacement behavior on the soft-tissue restraints. Additionally, this adjustment leaves the soft-tissue restraints as the only source for internal joint force (Figure 3.1), and this may lead to an improved estimation of ligament properties. This work uses novel experimental loading conditions in an inverse modeling scheme that is similar to previous studies (Blankevoort and Huiskes, 1996; Baldwin et al., 2012; Ewing et al., 2015; Harris et al., 2016) to estimate ligament slack lengths. This work focused on estimating slack length because Baldwin et al. (2009) showed that passive joint kinematics are more sensitive to ligament slack length than stiffness. The purpose of this work was to use novel experimental loading in an inverse modeling scheme to estimate ligament slack lengths.

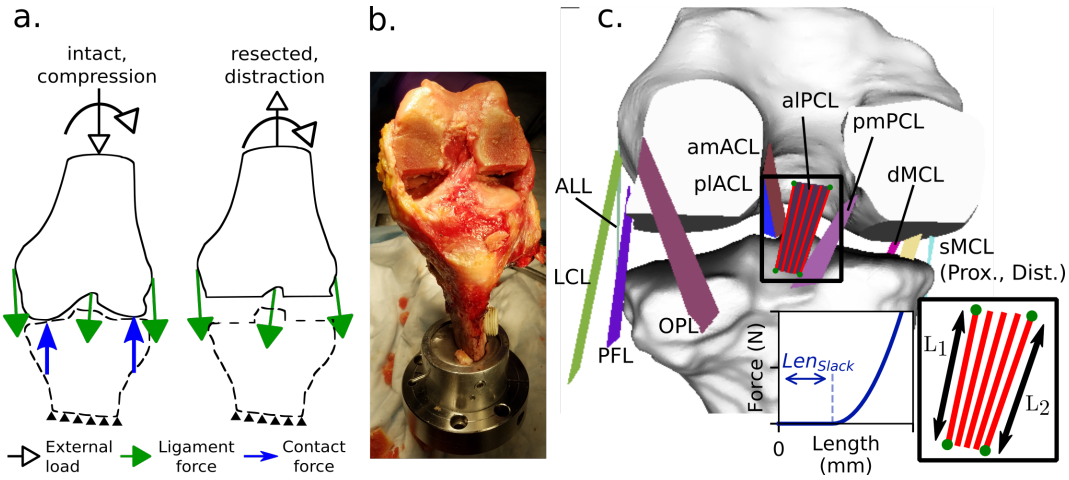

Figure 3.1: (a) A similified representation of the joint forces during an intact laxity-style test compared to a distraction laxity-style test. (b) The specimen with resected femoral articulating surfaces. (c) The knee model with 11 ligament bundles represented. (inset) The non-linear spring model, and the definition of slack lenghth for a ligament with five fibers.

3.2 Methods

Specimen-specific geometry was defined using the specimen's MR images. The femur and the tibia were segmented, and 11 ligament bundles were defined using the MR images and literature descriptions (Figure 3.1). The anterior and posterior cruciate ligaments were modeled as four bundles. These bundles were the anteromedial and posterolateral anterior cruciate ligament (amACL, plACL) (Duthon et al., 2006) and the anterolateral and posteromedial posterior cruciate ligament (alPCL, pmPCL) (Anderson et al., 2012). The medial collateral ligament (MCL) was modeled as three bundles. Two of those bundles composed the proximal and distal superficial MCL (psMCL, dsMCL), and one bundle defined the deep MCL (dMCL) (LaPrade, 2007b). Additional ligament bundles included the lateral collateral ligament (LCL), the popliteofibular ligament (PFL) (LaPrade et al., 2003), the anterolateral ligament (ALL) (Claes et al., 2013), and the oblique popliteal ligament (OPL) (LaPrade, 2007a; Hedderwick et al., 2017).

The ligament bundles were defined by manually placing two points at the margins of femoral and tibial insertion sites (four points total). Each bundle consisted of 25 fibers, where two fibers connect the points that define the insertion area, and the remaining 23 fibers are evenly mapped between the margins. Each ligament fiber was modeled as a nonlinear spring (Blankevoort and Huiskes (1996)). Uniform stiffness was applied across each ligament, where the fiber stiffnesses summed to the ligament's equivalent stiffness (Table 3.1).

Experimental kinetics were applied to the forward kinematics model, and the length of each ligament fiber was used to calculate the magnitude of force carried by each fiber. The line of action was defined using each fiber's femoral and tibial insertion point. Based on visualization of the kinematics, some ligaments

Table 3.1: The equivalent stiffness (N/ϵ) of each ligament bundle with units of force per unit strain.

Ligament	**Stiffness**	**Reference**
amACL	2120	Amiri et al. (2007), Kia et al. (2016)
plACL	2880	Amiri et al. (2007), Kia et al. (2016)
alPCL	5625	Amiri et al. (2007), Kia et al. (2016)
pmPCL	3375	Amiri et al. (2007), Kia et al. (2016)
psMCL	1375	Amiri et al. (2007)
dsMCL	1375	Amiri et al. (2007)
dMCL	1000	Amiri et al. (2007)
LCL	2000	Amiri et al. (2007)
ALL	750	Ewing et al. (2015)
PFL	1000	Ewing et al. (2015)
OPL	1000	Ewing et al. (2015)

simulated wrapping around either the femur, or a cylinder that approximated the tibia's surface. Tibial reaction forces were calculated by summing the force carried by each ligament fiber along its line of action (Mommersteeg et al., 1996), and when applicable, the wrapping reaction forces. Tibial reaction moments were calculated with tibial insertion points, wrapping points, and each fiber's force magnitude and line of action.

Ligament slack lengths were estimated using a constrained sequential quadratic programming algorithm. To simulate nonhomogeneous prestrain, two values were used to define ligament slack length for every fiber in a ligament bundle. The length of the two fibers at the margins of the insertion site was defined, and linear interpolation was used to define the slack length for the remaining fibers (Figure 3.1). The optimization minimized the residual between the model and experimentally measured tibial reaction forces for the anterior-posterior drawer and fixed varus-valgus distraction tests at 0°, 30°, 60°, 90° flexion (Equation 3.1).

$$\begin{aligned} &\underset{\boldsymbol{x}}{\text{minimize}} && f(\boldsymbol{x}) = \sum_{j=1}^{72} \sum_{j=1}^{6} \left[w_j (M_{ij}(\boldsymbol{x}) - E_{ij}) \right]^2 \\ &\text{subject to} \\ & && h(x_m) \geq 0.1,\ m = 1, \ldots, 22 \end{aligned} \tag{3.1}$$

Where i is number of the step in the loading cycle, and j is the force degree of freedom. The weighting factor (w) applied a weight of 1 to the forces, and a weight of 20 to the moments. Three experimental tests were excluded from the optimization to evaluate the inverse modeling scheme's performance.

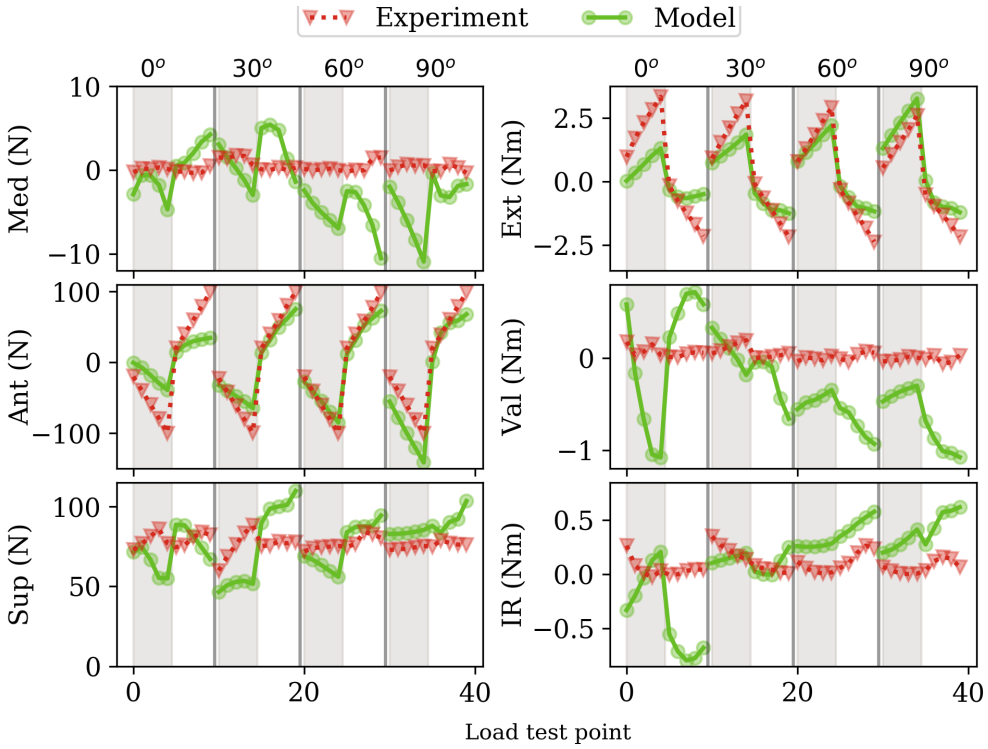

Figure 3.2: Tibial reaction forces and moments for the (grey) anterior and (white) posterior drawer tests for the experiment and calibrated model at 0°, 30°, 60°, 90° flexion. Med, Ant, Sup are the medial, anterior, and superior tibial reaction forces, respectively. Ext, Val, IR are the extension, valgus, and internal tibial rotation reaction moments, respectively.

3.3 Results and Discussion

For the tests that were included in the optimization (anterior-posterior drawer and varus-valgus), the RMS error of the joint kinetics across all flexion angles was 5.8 N, 22.5 N and 17.1 N for the medial, anterior, and superior loads respectively, and 0.80 Nm, 0.60 Nm, and 0.33 Nm for the extension, valgus, and internal rotation moments respectively (Figure 3.2, Figure 3.3).

For the distraction test, which was not part of the optimization, the RMS error of the joint kinetics across all flexion angles was 2.5 N, 13.4 N and 14.2 N for the medial, anterior, and superior loads respectively, and 0.54 Nm, 0.36 Nm, and 0.31 Nm for the extension, valgus, and internal rotation moments respectively (Figure 3.4).

For the kinetic plane and distraction tests, the highest errors in anterior force occurred at 90° flexion, and the highest distraction force errors occurred at 0° flexion (Table 3.2). The internal-external rotation model demonstrated the largest difference in distraction force (Table 3.2). For the internal-external rotation tests, the model performed better when the applied torque was lower. Across flexion angles, the RMS distraction force error was 13.5 N at ± 1 Nm internal rotation torque, and 46.2 N at ± 5 Nm internal rotation torque.

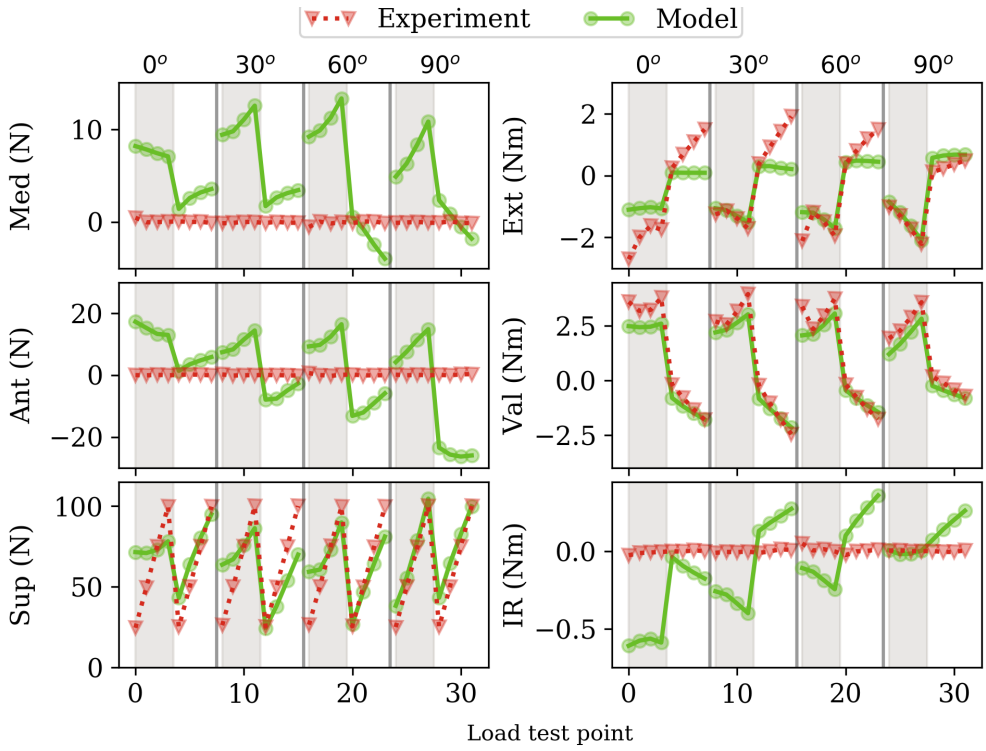

Figure 3.3: Tibial reaction forces and moments for the (grey) varus and (white) valgus tests for the experiment and calibrated model at 0°, 30°, 60°, 90° flexion. Med, Ant, Sup are the medial, anterior, and superior tibial reaction forces, respectively. Ext, Val, IR are the extension, valgus, and internal tibial rotation reaction moments, respectively.

Table 3.2: RMS errors between the experimental and calibrated model joint reaction forces (N) and moments (Nm) for the distraction, kinetic plane, and external-internal rotation tests. These tests were not part of the optimization.

Flexion	**Test**	F_{med}	F_{ant}	F_{sup}	M_{ext}	M_{val}	M_{ir}
0°	K. Pl.	9.87	19.29	10.47	1.06	0.18	0.66
	Dist.	0.46	11.64	18.68	0.64	0.16	0.50
	ER	2.73	11.94	13.41	1.00	0.21	2.72
	IR	3.67	20.99	28.32	2.00	0.93	3.32
30°	K. Pl.	11.84	11.07	9.85	1.01	0.17	0.07
	Dist.	4.19	6.63	12.48	0.69	0.20	0.01
	ER	3.60	9.03	32.09	0.94	0.99	2.86
	IR	6.07	36.09	45.38	1.25	0.34	3.24
60°	K. Pl.	8.65	6.45	9.09	0.42	0.44	0.37
	Dist.	2.41	4.42	9.13	0.17	0.42	0.29
	ER	0.81	9.70	53.11	0.61	0.60	3.02
	IR	2.30	13.58	59.35	0.82	0.29	3.24
90°	K. Pl.	7.58	25.15	7.99	0.72	0.65	0.30
	Dist.	0.87	22.71	14.62	0.50	0.51	0.22
	ER	5.58	6.43	43.39	0.93	0.45	2.72
	IR	3.66	18.70	33.68	0.33	0.36	2.71

K. Pl.: kinetic plane test, Dist.: distraction test, ER.: external tibial rotation test, IR.: internal tibial rotation test.
F_{med}, F_{ant}, F_{sup}: medial, anterior and superior tibial reaction forces, respectively.
M_{ext}, M_{val}, M_{ir}: extension, valgus, and internal tibial rotation tibial reaction moments, respectively.

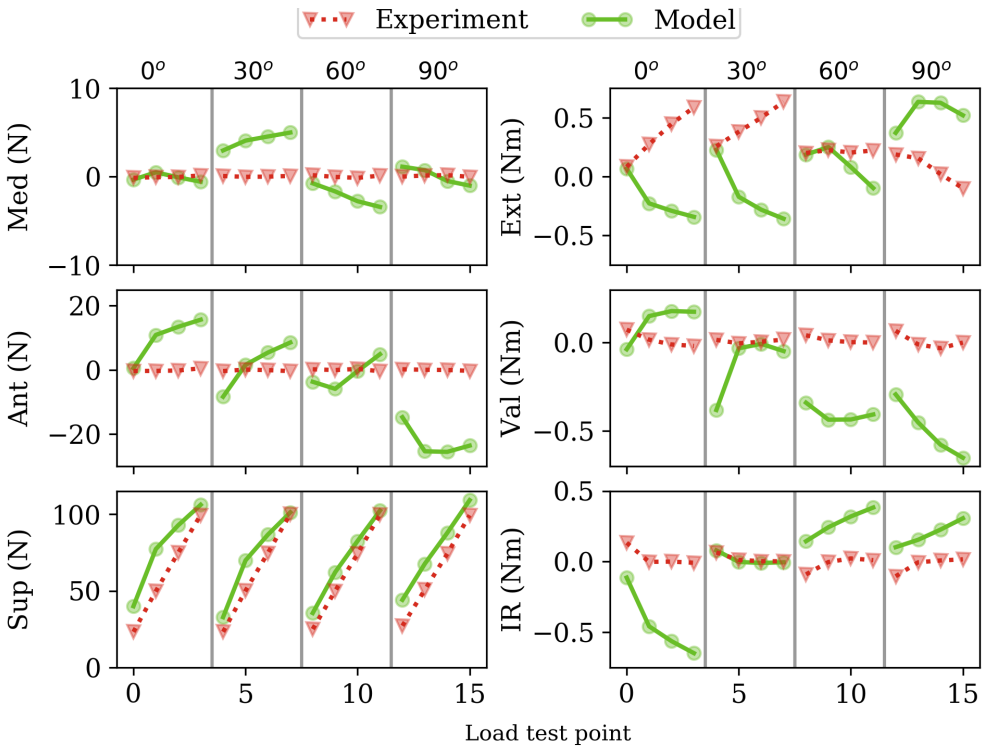

Figure 3.4: Tibial reaction forces and moments for the calibrated model compared to the experimentally measured values for the distraction test. Results are shown for 0°, 30°, 60°, 90° flexion. This test was not included in the optimization. Med, Ant, Sup are the medial, anterior, and superior tibial reaction forces, respectively. Ext, Val, IR are the extension, valgus, and internal tibial rotation reaction moments, respectively.

Chapter 4

Inverse Modeling

4.1 Introduction

Ligament geometry is defined from MR images where the ligament is under an unknown amount of load.

4.2 Methods

Chapter 5

Bibliography

Bibliography

Azhar A. Ali, Sami S. Shalhoub, Adam J. Cyr, Clare K. Fitzpatrick, Lorin P. Maletsky, Paul J. Rullkoetter, and Kevin B. Shelburne. Validation of predicted patellofemoral mechanics in a finite element model of the healthy and cruciate-deficient knee. *Journal of Biomechanics*, 49(2):302–309, January 2016. ISSN 0021-9290. doi: 10.1016/j.jbiomech.2015.12.020. URL http://www.sciencedirect.com/science/article/pii/S0021929015007265.

S. Amiri, D. Cooke, I. Y. Kim, and U. Wyss. Mechanics of the passive knee joint. Part 2: interaction between the ligaments and the articular surfaces in guiding the joint motion. *Proceedings of the Institution of Mechanical Engineers Part H-Journal of Engineering in Medicine*, 221(H8):821–832, November 2007. ISSN 0954-4119. doi: 10.1243/09544119JEIM181. WOS:000251718000001.

Shahram Amiri, David R. Wilson, Shahram Amiri, and David R. Wilson. A Computational Modeling Approach for Investigating Soft Tissue Balancing in Bicruciate Retaining Knee Arthroplasty. *Computational and Mathematical Methods in Medicine, Computational and Mathematical Methods in Medicine*, 2012:652865, October 2012. ISSN 1748-670X, 1748-670X. doi: 10.1155/2012/652865,10.1155/2012/652865. URL http://www.hindawi.com/journals/cmmm/2012/652865/abs/,http://www.hindawi.com/journals/cmmm/2012/652865/abs/.

Colin J Anderson, Connor G Ziegler, Coen A Wijdicks, Lars Engebretsen, and Robert F LaPrade. Arthroscopically Pertinent Anatomy of the Anterolateral and Posteromedial Bundles of the Posterior Cruciate Ligament. *The Journal of Bone and Joint Surgery-American Volume*, 94(21):1936–1945, November 2012. ISSN 0021-9355. doi: 10.2106/JBJS.K.01710. URL http://content.wkhealth.com/linkback/openurl?sid=WKPTLP:landingpage&an=00004623-201211070-00003.

Mark Baldwin, Peter Laz, Joshua Stowe, and Paul Rullkoetter. Efficient probabilistic representation of tibiofemoral soft tissue constraint. *Computer Methods in Biomechanics and Biomedical Engineering*, 12 (6):651–659, December 2009. doi: 10.1080/10255840902822550.

Mark A. Baldwin, Chadd W. Clary, Clare K. Fitzpatrick, James S. Deacy, Lorin P. Maletsky, and Paul J. Rullkoetter. Dynamic finite element knee simulation for evaluation of knee replacement mechanics. *Journal of Biomechanics*, 45(3):474–483, February 2012. ISSN 0021-9290. doi: 10.1016/j.jbiomech.2011.11.052. URL http://www.sciencedirect.com/science/article/pii/S0021929011007469.

Hamid Naghibi Beidokhti, Dennis Janssen, Sebastiaan van de Groes, Javad Hazrati, Ton Van den Boogaard, and Nico Verdonschot. The influence of ligament modelling strategies on the predictive capability of finite element models of the human knee joint. *Journal of Biomechanics*, 65:1–11, December 2017. ISSN 0021-9290, 1873-2380. doi: 10.1016/j.jbiomech.2017.08.030. URL http://www.jbiomech.com/article/S0021-9290(17)30452-9/abstract.

L. Blankevoort and R. Huiskes. Ligament-bone interaction in a three-dimensional model of the knee. *Journal of Biomechanical Engineering*, 113(3):263–269, 1991. URL http://biomechanical.asmedigitalcollection.asme.org/article.aspx?articleid=1398621.

L. Blankevoort and R. Huiskes. Validation of a three-dimensional model of the knee. *Journal of Biomechanics*, 29(7):955–961, July 1996. ISSN 0021-9290. doi: 10.1016/0021-9290(95)00149-2. URL http://www.sciencedirect.com/science/article/pii/0021929095001492.

Steven Claes, Evie Vereecke, Michael Maes, Jan Victor, Peter Verdonk, and Johan Bellemans. Anatomy of the anterolateral ligament of the knee. *Journal of Anatomy*, 223(4):321–328, October 2013. ISSN 1469-7580. doi: 10.1111/joa.12087. URL http://onlinelibrary.wiley.com/doi/10.1111/joa.12087/abstract.

Yasin Y. Dhaher, Tae-Hyun Kwon, and Megan Barry. The effect of connective tissue material uncertainties on knee joint mechanics under isolated loading conditions. *Journal of Biomechanics*, 43 (16):3118–3125, December 2010. ISSN 0021-9290. doi: 10.1016/j.jbiomech.2010.08.005. URL http://www.sciencedirect.com/science/article/pii/S0021929010004380.

V. B. Duthon, C. Barea, S. Abrassart, J. H. Fasel, D. Fritschy, and J. Mntrey. Anatomy of the anterior cruciate ligament. *Knee Surgery, Sports Traumatology, Arthroscopy*, 14(3):204–213, March 2006. ISSN 0942-2056, 1433-7347. doi: 10.1007/s00167-005-0679-9. URL http://link.springer.com/article/10.1007/s00167-005-0679-9.

Ahmet Erdemir. Open Knee: Open Source Modeling & Simulation to Enable Scientific Discovery and Clinical Care in Knee Biomechanics. *The journal of knee surgery*, 29(2):107–116, February 2016. ISSN 1538-8506. doi: 10.1055/s-0035-1564600. URL https://www.ncbi.nlm.nih.gov/pmc/articles/PMC4876308/.

Joseph A. Ewing, Michelle K. Kaufman, Erin E. Hutter, Jeffrey F. Granger, Matthew D. Beal, Stephen J. Piazza, and Robert A. Siston. Estimating patient-specific soft-tissue properties in a TKA knee. *Journal of Orthopaedic Research*, pages 435–443, September 2015. ISSN 1554-527X. doi: 10.1002/jor.23032. URL http://onlinelibrary.wiley.com/doi/10.1002/jor.23032/abstract.

Benjamin J. Fregly, Scott A. Banks, Darryl D. D'Lima, and Clifford W. Colwell. Sensitivity of knee replacement contact calculations to kinematic measurement errors. *Journal of Orthopaedic Research*, 26(9): 1173–1179, September 2008. ISSN 1554-527X. doi: 10.1002/jor.20548. URL http://onlinelibrary.wiley.com/doi/10.1002/jor.20548/abstract.

J. C. Gardiner, J. A. Weiss, and T. D. Rosenberg. Strain in the human medial collateral ligament during valgus loading of the knee. *Clinical Orthopaedics and Related Research*, (391):266–274, October 2001. ISSN 0009-921X. WOS:000171523600032.

John C. Gardiner and Jeffrey A. Weiss. Subject-specific finite element analysis of the human medial collateral ligament during valgus knee loading. *Journal of Orthopaedic Research*, 21(6):1098–1106, January 2003. ISSN 0736-0266. doi: 10.1016/S0736-0266(03)00113-X. URL http://www.sciencedirect.com/science/article/pii/S073602660300113X.

Michael D. Harris, Adam J. Cyr, Azhar A. Ali, Clare K. Fitzpatrick, Paul J. Rullkoetter, Lorin P. Maletsky, and Kevin B. Shelburne. A Combined Experimental and Computational Approach to Subject-Specific Analysis of Knee Joint Laxity. *Journal of Biomechanical Engineering*, 138(8):081004–081004, June 2016. ISSN 0148-0731. doi: 10.1115/1.4033882. URL http://dx.doi.org/10.1115/1.4033882.

Mandy Hedderwick, Mark D. Stringer, Liam McRedmond, Grant R. Meikle, and Stephanie J. Woodley. The oblique popliteal ligament: an anatomic and MRI investigation. *Surgical and Radiologic Anatomy*, 39(9):1017–1027, September 2017. ISSN 0930-1038, 1279-8517. doi: 10.1007/s00276-017-1838-7. URL http://link.springer.com/10.1007/s00276-017-1838-7.

M. L. Hull, Gregory S. Berns, H. Varma, and Hugh A. Patterson. Strain in the medial collateral ligament of the human knee under single and combined loads. *Journal of Biomechanics*, 29(2):199–206, February 1996. ISSN 0021-9290. doi: 10.1016/0021-9290(95)00046-1. URL http://www.sciencedirect.com/science/article/pii/0021929095000461.

Mohammad Kia, Kevin Schafer, Joseph Lipman, Michael Cross, David Mayman, Andrew Pearle, Thomas Wickiewicz, and Carl Imhauser. A Multibody Knee Model Corroborates Subject-Specific Experimental Measurements of Low Ligament Forces and Kinematic Coupling During Passive Flexion. *Journal of*

Biomechanical Engineering, 138(5):051010–1–051010–12, March 2016. ISSN 0148-0731. doi: 10.1115/1.4032850. URL http://dx.doi.org/10.1115/1.4032850.

Robert F. LaPrade. The Anatomy of the Posterior Aspect of the Knee: An Anatomic Study. *The Journal of Bone and Joint Surgery (American)*, 89(4):758–764, April 2007a. ISSN 0021-9355. doi: 10.2106/JBJS.F.00120. URL http://jbjs.org/cgi/doi/10.2106/JBJS.F.00120.

Robert F. LaPrade. The Anatomy of the Medial Part of the Knee. *The Journal of Bone and Joint Surgery (American)*, 89(9):2000–2010, September 2007b. ISSN 0021-9355. doi: 10.2106/JBJS.F.01176. URL http://jbjs.org/cgi/doi/10.2106/JBJS.F.01176.

Robert F. LaPrade, Thuan V. Ly, Fred A. Wentorf, and Lars Engebretsen. The posterolateral attachments of the knee. *The American Journal of Sports Medicine*, 31(6):854–860, 2003. URL http://journals.sagepub.com/doi/abs/10.1177/03635465030310062101.

G. Limbert, M. Taylor, and J. Middleton. Three-dimensional finite element modelling of the human ACL: simulation of passive knee flexion with a stressed and stress-free ACL. *Journal of Biomechanics*, 37 (11):1723–1731, November 2004. ISSN 0021-9290. doi: 10.1016/j.jbiomech.2004.01.030. URL http://www.sciencedirect.com/science/article/pii/S0021929004000740.

Jia Lu, Xianlian Zhou, and Madhavan L. Raghavan. Computational method of inverse elastostatics for anisotropic hyperelastic solids. *International Journal for Numerical Methods in Engineering*, 69(6):1239–1261, February 2007. ISSN 1097-0207. doi: 10.1002/nme.1807. URL https://onlinelibrary.wiley.com/doi/abs/10.1002/nme.1807.

Steve A. Maas, Ahmet Erdemir, Jason P. Halloran, and Jeffrey A. Weiss. A general framework for application of prestrain to computational models of biological materials. *Journal of the Mechanical Behavior of Biomedical Materials*, 61:499–510, August 2016. ISSN 1751-6161. doi: 10.1016/j.jmbbm.2016.04.012. URL http://www.sciencedirect.com/science/article/pii/S1751616116300765.

T. J. A. Mommersteeg, L. Blankevoort, R. Huiskes, J. G. M. Kooloos, and J. M. G. Kauer. Characterization of the mechanical behavior of human knee ligaments: A numerical-experimental approach. *Journal of Biomechanics*, 29(2):151–160, February 1996. ISSN 0021-9290. doi: 10.1016/0021-9290(95)00040-2. URL http://www.sciencedirect.com/science/article/pii/0021929095000402.

G. A. Orozco, P. Tanska, M. E. Mononen, K. S. Halonen, and R. K. Korhonen. The effect of constitutive representations and structural constituents of ligaments on knee joint mechanics., The effect of constitutive representations and structural constituents of ligaments on knee joint mechanics. *Scientific reports,*

Scientific Reports, 8, 8(1):2323–2323, 2018. ISSN 2045-2322. doi: 10.1038/s41598-018-20739-w,10.1038/s41598-018-20739-w. URL http://europepmc.org/abstract/MED/29396466,http://europepmc.org/articles/PMC5797142/?report=abstract.

E. Pea, B. Calvo, M. A. Martnez, and M. Doblar. A three-dimensional finite element analysis of the combined behavior of ligaments and menisci in the healthy human knee joint. *Journal of Biomechanics*, 39(9):1686–1701, January 2006. ISSN 0021-9290, 1873-2380. doi: 10.1016/j.jbiomech.2005.04.030. URL http://www.jbiomech.com/article/S0021-9290(05)00211-3/abstract.

H. H. Rachmat, D. Janssen, G. J. Verkerke, R. L. Diercks, and N. Verdonschot. In-situ mechanical behavior and slackness of the anterior cruciate ligament at multiple knee flexion angles. *Medical Engineering & Physics*, 38(3):209–215, March 2016. ISSN 1350-4533. doi: 10.1016/j.medengphy.2015.11.011. URL http://www.sciencedirect.com/science/article/pii/S1350453315002696.

Shahab Salehghaffari and Yasin Y. Dhaher. A phenomenological contact model: Understanding the graft-tunnel interaction in anterior cruciate ligament reconstructive surgery. *Journal of Biomechanics*, 48(10):1844–1851, July 2015. ISSN 0021-9290. doi: 10.1016/j.jbiomech.2015.04.034. URL http://www.sciencedirect.com/science/article/pii/S0021929015002547.

Colin R. Smith, Rachel L. Lenhart, Jarred Kaiser, Michael F. Vignos, and Darryl G. Thelen. Influence of Ligament Properties on Tibiofemoral Mechanics in Walking. *Journal of Knee Surgery*, 29(2):99–106, February 2016a. ISSN 1538-8506. doi: 10.1055/s-0035-1558858. WOS:000373292000003.

Colin R. Smith, Michael F. Vignos, Rachel L. Lenhart, Jarred Kaiser, and Darryl G. Thelen. The Influence of Component Alignment and Ligament Properties on Tibiofemoral Contact Forces in Total Knee Replacement. *Journal of Biomechanical Engineering*, 138(2):021017–1–021017–10, January 2016b. ISSN 0148-0731. doi: 10.1115/1.4032464. URL http://dx.doi.org/10.1115/1.4032464.

Yuhua Song, Richard E. Debski, Volker Musahl, Maribeth Thomas, and Savio L. Y. Woo. A three-dimensional finite element model of the human anterior cruciate ligament: a computational analysis with experimental validation. *Journal of Biomechanics*, 37(3):383–390, March 2004. ISSN 0021-9290. doi: 10.1016/S0021-9290(03)00261-6. URL http://www.sciencedirect.com/science/article/pii/S0021929003002616.

Julie A. Thompson, Michael W. Hast, Jeffrey F. Granger, Stephen J. Piazza, and Robert A. Siston. Biomechanical Effects of Total Knee Arthroplasty Component Malrotation: A Computational Simula-

tion. *Journal of Orthopaedic Research*, 29(7):969–975, July 2011. ISSN 0736-0266. doi: 10.1002/jor.21344. WOS:000290632900001.

Peter S. Walker, Michael T. Lowry, and Anoop Kumar. The Effect of Geometric Variations in Posterior-stabilized Knee Designs on Motion Characteristics Measured in a Knee Loading Machine. *Clinical Orthopaedics and Related Research*, 472(1):238–247, January 2014. ISSN 0009-921X, 1528-1132. doi: 10.1007/s11999-013-3088-2. URL `http://link.springer.com/10.1007/s11999-013-3088-2`.

J. A. Weiss and J. C. Gardiner. Computational modeling of ligament mechanics. *Critical Reviews in Biomedical Engineering*, 29(3):303–371, 2001. ISSN 0278-940X.

Jiang Yao, Arthur D. Salo, Jordan Lee, and Amy L. Lerner. Sensitivity of tibio-menisco-femoral joint contact behavior to variations in knee kinematics. *Journal of Biomechanics*, 41(2):390–398, January 2008. ISSN 0021-9290. doi: 10.1016/j.jbiomech.2007.08.015. URL `http://www.sciencedirect.com/science/article/pii/S0021929007003739`.